JOURNAL OF APPLIED ELECTROCHEMISTRY 24 (1994) 1092–1101

Electrochemical polishing of hydrogen sulfide from coal synthesis gas

S. R. ALEXANDER*, J. WINNICK

School of Chemical Engineering, Georgia Institute of Technology, Atlanta, GA 30332-0100, USA

Received 13 May 1993; revised 28 March 1994

An advanced process has been developed for the separation of H_2S from coal gasification product streams through an electrochemical membrane. This technology is developed for use in coal gasification facilities providing fuel for cogeneration coal fired electrical power facilities and molten carbonate fuel cell (MCFC) electrical power facilities. H_2S is removed from the syn-gas by reduction to the sulfide ion and hydrogen gas at the cathode. The sulfide ion migrates to the anode through a molten salt electrolyte suspended in an inert ceramic matrix. Once at the anode it is oxidized to elemental sulfur and swept away for condensation in an inert gas stream. The syn-gas is enriched with the hydrogen. Order of magnitude reductions in H_2S have been repeatedly recorded (100 ppm to 10 ppm H_2S) on a single pass through the cell. This process allows removal of H_2S without cooling the gas stream and with negligible pressure loss through the separator. Since there are no absorbents used, there is no absorption/regeneration step as with conventional technology. Elemental sulfur is produced as a byproduct directly, so there is no need for a Claus process for sulfur recovery. This makes the process economically attractive since it is much less equipment intensive than conventional technology.

1. Introduction

Use of selective membranes for separating gaseous components from mixtures is a common unit operation. The thermodynamic basis for separation is very simple: a component will only move down a chemical potential gradient, $\Delta\mu$:

$$\Delta\mu_i = \mu_i - \mu_i' = RT\ln(a_i/a_i') \qquad (1)$$

where the prime $'$ refers to the extracted phase and a_i refers to the activity of component i. Thus, for a separation from a phase with 1% into a pure phase, a minimum pressure ratio of about 100 is needed. In actual practice a higher pressure drop is needed to promote a significant flux. These processes do not produce a high-purity product, nor do they remove one component with perfect selectivity.

The situation is different for a charged species in the presence of an electric potential, $\Delta\phi$. Here, the electrochemical potential, μ, is the driving force:

$$\Delta\bar{\mu}_i = \bar{\mu}_i - \bar{\mu}_i' = RT\ln(a_i/a_i') + z_iF\Delta\Phi \qquad (2)$$

So, for a species with a charge of ±2, a potential difference of 0.06 V can maintain the same concentration difference that requires 100 atm for an uncharged species. The effect is more pronounced as the concentration in the feed drops to levels encountered in contaminant removal, e.g. 10 ppm. Here a pressure driven separation to a pure stream would require more than 10^5 atm while an electrochemical separation requires only 0.15 V [1].

This principle has been applied to high temperature gas mixtures including H_2S in nitrogen [2], sour coal gas (H_2S levels greater than 1000 ppm) [3], and natural gas (H_2S levels from 1.3% to 100 ppm) [4]. The primary gaseous pollutant in each of these cases has been H_2S in a fuel gas stream, but removal of SO_2 has also been achieved from flue gas streams [5]. The membrane is exposed to the same pressure on both sides, so there is no theoretical limit to the pressure at which the process can operate. The main thrust of this paper is polishing H_2S from coal synthesis gas (H_2S levels of 100 ppm and less).

2. Technical discussion

The major gaseous contaminant in raw coal gas is H_2S. Much of the coal reserves in the United States contain up to 5 wt % sulfur, which is converted to H_2S during gasification. The H_2S concentration (and raw coal gas composition) depends on the type of coal and the gasification conditions, but levels from 0.5 to 1.0 volume percent are typical (see Table 1 for a listing of some representative compositions [6]). Before this gas can be used for power generation, the H_2S concentration must be reduced to 100 ppm or less (MCFC plants require concentrations of no more than 1 ppm H_2S). Conventional processes to remove H_2S rely on low to ambient temperature absorption, followed by sorbent regeneration and

---

* Presently at the Hoechst Celanese Corporation, Corpus Christi Technical Center, 1901 Clarkwood Rd., P.O. Box 9077, Corpus Christi, TX 78469, (512) 242–4000, USA

*Table 1. Representative coal gas compositions**

CO	15–30%
CO_2	4–25%
H_2	12–59%
N_2	0–59%
CH_4	2–19%
H_2S	0.5–1.5%

* Dry basis.

Claus treatment for conversion of concentrated H_2S to elemental sulfur [7].

A hot gas electrochemical membrane process for the removal of H_2S is illustrated schematically in Fig. 1. The process gas is passed by the cathode; here, the most easily reduced component, that is, the strongest Lewis acid, will be reduced. In many mixtures of sour gas, this is H_2S:

$$H_2S + 2e^- \longrightarrow H_2 + S^{2-} \tag{3}$$

A membrane which contains sulfide ions in a molten state acts to transport sulfide across to the anode where, in the simplest case, hydrogen can be supplied to form H_2S. Alternatively, an inert sweep gas such as nitrogen can be used at the anode to carry away oxidized sulfide ions as vaporous sulfur.

The situation can become complicated when coal gas mixtures are processed. Carbon dioxide and water compete in the reduction reaction by

$$CO_2 + H_2O + 2e^- \longrightarrow CO_3^{2-} + H_2 \tag{4}$$

The ionic flux through the membrane depends upon the relative mobilities of carbonate and sulfide as well as their concentrations.

From the equilibrium constant for Reaction 5 below, it is possible to know the electrolyte composition which would be in equilibrium with a given process gas at a given process temperature. Theoretical membrane electrolyte compositions are calculated by thermodynamic analysis of equilibrium, Reaction 5. Since membranes similar to those used in the MCFC were used in these studies, the cations present were of potasssium and lithium in a ratio corresponding to the low melting carbonate eutectic ($Li_{0.62}K_{0.38}$):

$$\begin{aligned}&(Li_{0.62}K_{0.38})_2CO_3 + H_2S\\ &\quad = (Li_{0.62}K_{0.38})_2S + CO_2 + H_2O\end{aligned} \tag{5}$$

This analysis was performed by finding the Gibbs energy change of Reaction 5 at the process temperature and relating this to the equilibrium constant, K_a, with K_a defined as

Table 2. Calculated and experimental equilibrium electrolyte compositions

Mol % sulfide	
Calculated	*Experimental*
2.6	3.5
6.4	4.2
11.3	16.7
13.5	15.8
18.1	20.3
21.3	20.3
45.8	52.2

$$K \equiv \frac{p_{CO_2} p_{H_2O} a_{S^{2-}}}{p_{H_2S} a_{CO_3^{2-}}} \tag{6}$$

If the activity coefficients, γ, of the molten phase constituents (namely the sulfide and carbonate in the electrolyte) are assumed to be equal, then the activities of the molten phase constituents can be replaced by mole fractions (x_i):

$$K_a = \frac{p_{CO_2} p_{H_2O} x_{S^{2-}}}{p_{H_2S} x_{CO_3^{2-}}} \tag{7}$$

with

$$x_{M_2S} + x_{M_2CO_3} = 1 \tag{8}$$

By this analysis, a process gas with a composition of 14.4% CO_2, 6.2% H_2O, and 100 ppm H_2S with a run temperature of 973 K will correspond to an electrolyte composition of 0.6% sulfide and 99.4% carbonate. Post-run quantitative chemical analysis of membranes used in these experiments has shown good agreement with predicted electrolyte sulfide levels. Table 2 shows a comparison of calculated equilibrium sulfide levels and the corresponding experimentally determined sulfide compositions.

The direct oxidation of carbonate:

$$CO_3^{2-} \longrightarrow CO_2 + \tfrac{1}{2}O_2 + 2e^- \tag{9}$$

occurs at a standard potential some 0.70 V more positive than that for sulfide:

$$S^{2-} \longrightarrow \tfrac{1}{2}S_2 + 2e^- \tag{10}$$

When the half-cell reactions (3) and (10) are summed, the resulting cell reaction and standard potential at

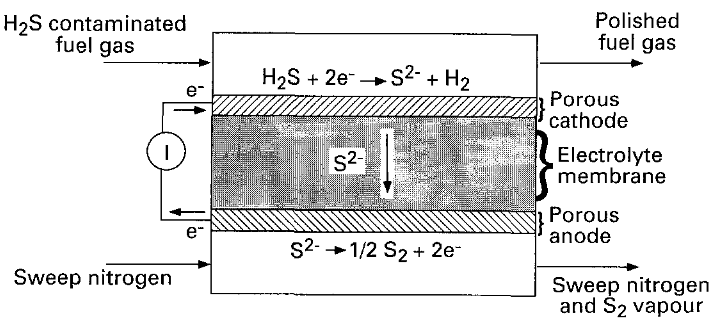

Fig. 1. Electrochemical coal gas desulfurization cell.

900 K are

$$H_2S \longrightarrow H_2 + \tfrac{1}{2}S_2 \quad \text{for } E^0 = -0.239\,\text{V} \qquad (11)$$

and when the half-cell reactions (4) and (9) are summed, the resulting cell reaction and standard potential are

$$H_2O \longrightarrow H_2 + \tfrac{1}{2}O_2 \quad \text{for } E^0 = -1.030\,\text{V} \qquad (12)$$

This shows an electrochemical potential 'window of operation' between the two cross cell reactions. If the cross-cell potential (cathode to anode) with current applied to the cell is kept below the level required for the sulfide transport reaction (11) yet above the level required for the carbonate transport reaction (12), then sulfide is preferentially transported across the cell and H_2S preferentially removed from the process gas stream.

This preferential transport will be disrupted if hydrogen gas, even at low rates, permeates through the membrane from the cathode to the anode side. This hydrogen is then available for oxidation of carbonate;

$$H_2 + CO_3^{2-} = H_2O + CO_2 + 2e^- \qquad (13)$$

When this reaction is combined with Reaction 4, the standard potential falls to zero and the electrochemical window is thus closed; CO_2 will be transported preferentially to H_2S.

2.1. *Theoretical potentials and kinetics*

The equilibrium potential for combined reactions (3) and (10) is given by:

$$E = E^0 - \frac{RT}{2F}\ln\left[\frac{(p_{S_2})^{1/2}}{a_{S^{2-}}}\right]_{\text{anode}} - \frac{RT}{2F}\ln\left[\frac{p_{H_2}a_{S^{2-}}}{p_{H_2S}}\right]_{\text{cathode}} \qquad (14)$$

Additional voltage is required to run the separation cell due to irreversibilities. These losses originate from three sources: ohmic (η_{ohm}), concentration polarization (η_{conc}), and activation polarization (η_{act}) [8].

Several processes contribute to concentration polarization: mass transport through the bulk gas, diffusion in the gas phase through the electrode pores, solution/dissolution of reactants/products into/out of the electrolyte, and diffusion of reactants/products through the electrolyte to/from the electrochemical reaction site. However, analysis of the MCFC, with near-identical characteristics, shows the bulk-gas diffusion controls (e.g., [3]). In the present process, it is the rate of transport of H_2S to the electrode surface from the bulk gas which is limiting.

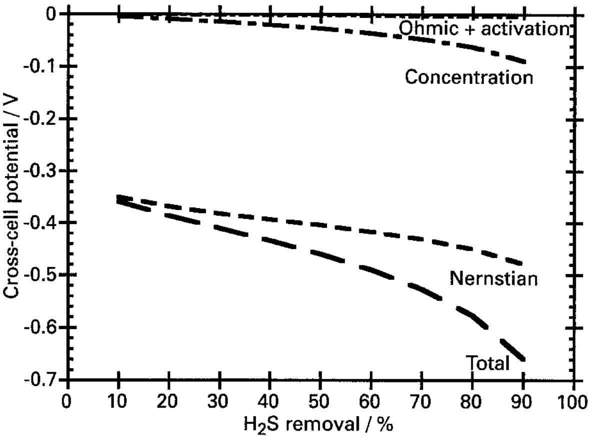

Fig. 2. Theoretical cross cell potential against % H_2S removal.

The thickness of the diffusion layer above the electrode surface, δ, is not well defined in this system. However, the limiting current density can be estimated using the average mass transfer coefficient, k_m, for the geometry involved. Thus, the estimation of the limiting current density becomes

$$i_L = nFk_m\rho\frac{(y_{\text{inlet}} - y_{\text{exit}})}{\ln(y_{\text{inlet}}/y_{\text{exit}})} \qquad (15)$$

where ρ is the molar density of the gas phase, y_{inlet} is the mole fraction of H_2S entering the removal cell, and y_{exit} is the mole fraction of H_2S exiting the cell. The average mass transfer coefficient, k_m, is given by the Sherwood number, an empirical term which has been tabulated for a variety of flow channel geometries and physical properties of the gas mixture [22].

The activation polarizations at the cathode and the anode of the cell are determined through the Butler–Volmer equation [23], requiring values for α_a, α_c, and i_o; these have been determined in previous experiments.

The lines presented in Fig. 2 were generated analytically using this approach. They are presented to demonstrate the relative magnitudes of the different components of the cell potential; they are merely an illustration of the expected cell polarizations in a hypothetical laboratory scale removal cell with a perfectly manufactured membrane. The conditions assumed consist of a cathodic flow rate of a coal synthesis gas equal to the anodic flow rate of nitrogen sweep gas ($0.0002\,\text{m}^3\,\text{min}^{-1}$), a system pressure of 1 atm, a run temperature of 898 K, and the polishing of H_2S from 100 ppm down to 10 ppm. The cathodic and anodic exchange current densities were estimated at $400\,\text{A}\,\text{m}^{-2}$ from the results of the free electrolyte studies performed by Banks [9] and White [10]. The exchange coefficients, α_a and α_c, were assumed to each be unity. Ohmic resistance across the cell was estimated to be $1\,\Omega$ [11]; and the superficial surface area of both the cathode and the anode was $0.000\,79\,\text{m}^2$ ($7.9\,\text{cm}^2$); the exposed active area was $0.000\,64\,\text{m}^2$ ($6.4\,\text{cm}^2$).

Examination of Fig. 2 shows that the calculated activation polarization at both the cathode and the anode is negligible. This shows extremely rapid electrochemical kinetics when compared to diffusion effects in the gas phase and in the electrolyte. All cross-cell potentials are shown to be due primarily to concentration polarization effects. Examination of this illustration shows that at 90% removal (100 ppm H_2S going to 10 ppm H_2S), a total cross-cell potential of about −0.660 V (cathode to anode) is expected.

Since the carbonate transport reaction is parallel to the sulfide transport reaction, some current to the cell will also act to transport CO_2 across the cell. The minimum required potential for this reaction is predicted by the Nernst equation for Reaction 12:

$$E = E^0 - \frac{RT}{2F}\left\{ \ln\left[\frac{p_{CO_2}(p_{O_2})^{1/2}}{a_{CO_3^{2-}}}\right]_{\text{anode}} + \ln\left[\frac{a_{CO_3^{2-}}p_{H_2}}{p_{CO_2}p_{H_2O}}\right]_{\text{cathode}} \right\} \tag{16}$$

This means that there is a maximum current efficiency with respect to H_2S removal for any given H_2S removal, depending on gas composition and the cross-cell potential required for the desired separation of H_2S. By solving the Nernst equation for carbonate transport, Reaction 16, at a given cross-cell potential with the known CO_2, H_2, and H_2O levels in the cathode gas, for the CO_2 and O_2 levels in the anode gas, the extent of this parallel carbonate transport reaction can be determined. This assumes that, in addition to rapid electrode kinetics, the concentration overpotential for CO_2 removal is negligible (a reasonable assumption since in this case the concentration is some three orders-of-magnitude higher for CO_2 and H_2O than for H_2S, with approximately 13% CO_2 and 3.3% H_2O in the cathode gas).

The extent of the anode CO_2 production with percentage H_2S removal is presented in Fig. 3; current efficiency is expected to drop to 35% at 90% H_2S removal. This means that, theoretically, applied current to the cell must be increased by a factor of about 3 over stoichiometric current to achieve this removal level. The excess current goes to reduction of CO_2 and H_2O at the cathode and production of anodic CO_2 and O_2. Even with a current efficiency of only 35%, power costs to perform this removal are negligible, as shown later.

Although the above analysis suggested that electrochemical polishing of H_2S from coal gas was possible, experiments were needed to verify that removal of H_2S from very low inlet levels could be attained in the presence of high concentrations of CO_2 and H_2O.

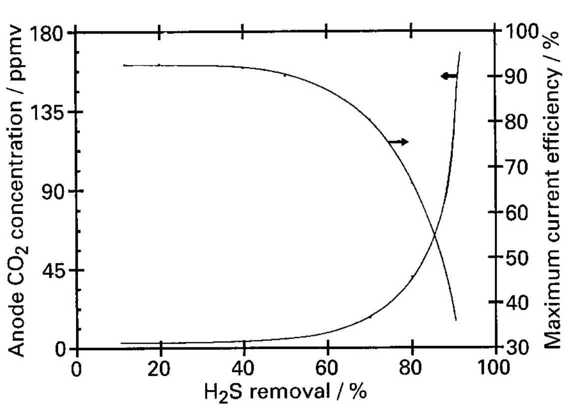

Fig. 3. Predicted anodic CO_2 production and maximum current efficiency against H_2S removal

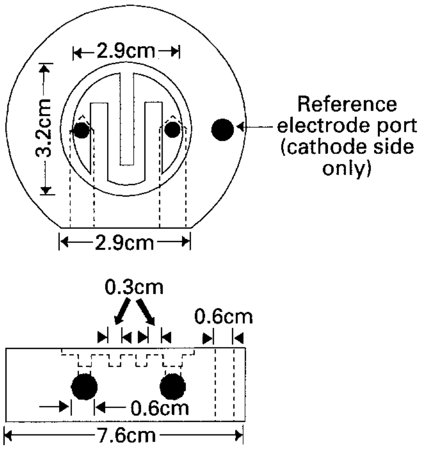

Fig. 4. Cell housing configuration.

3. Experimental methods

3.1. *Cell geometry*

The cell housings were machined from MACOR (machine ceramic) blocks. The housings were 0.076 m diameter and 0.025 m deep cylinders. Gas flow channels were machined into the large surface faces and gas flow tubes were connected to supply process and sweep gases to the cell (Fig. 4). Once the electrodes and membrane materials were ready for testing, the electrodes were set onto platinum current collectors placed on top of the gas flow channels on one side and contacting the membrane on the other (Fig. 5). The active superficial electrode area was 0.000 79 m^2 (7.9 cm^2), of which 0.000 64 m^2 (6.4 cm^2) was exposed to the process gas, the remainder occluded by the flow guides. The full cell was then assembled by placing the membrane between the MACOR blocks and connecting the gas supply lines to the assembly within a custom designed oven (Fig. 6). The arrangement is identical to that used previously [3]; although not shown, both gas analysers were used to analyze all gas inlet and outlet streams.

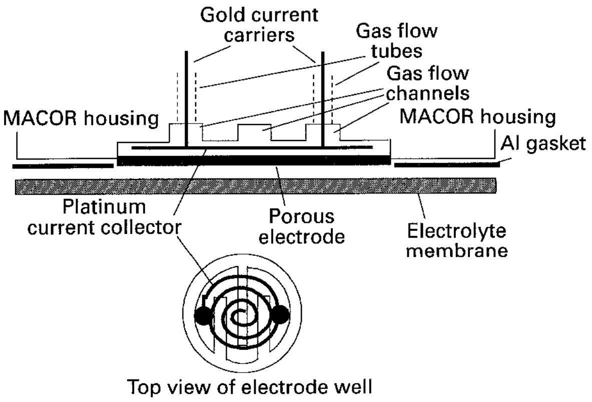

Fig. 5. Housing/current collector/electrode/gasket/membrane configuration.

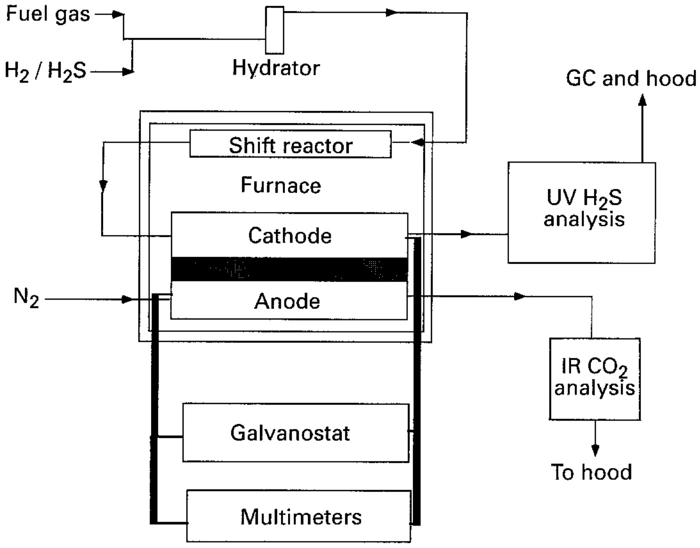

Fig. 6. Experimental apparatus configuration for coal gas polishing.

3.2. *Electrode preparation*

Weaver surveyed several possible electrode materials for this system [3, 12, 13]. Of these, lithiated Ni and NiO electrodes were used for this study. Nickel electrodes were donated to this research by ERC (Energy Research Corporation) as 0.20 m by 0.28 m sheets; average porosity was between 75 and 80%. A die was used to cut 0.032 m diameter electrodes from this sheet. These electrodes were then soaked in 1 M LiOH and then dried. When the nickel electrodes were used, the electrodes were then loaded into the cell and the run was started. If NiO electrodes were to be used, the electrodes were placed between two sintered Al_2O_3 sheets and loaded into an oven at 923 K under atmospheric air for at least six hours. Gravimetric analysis of these oxidized electrodes showed that the nickel was at least 96% converted to NiO.

3.3. *Membrane preparation*

The membrane between the two electrodes serves two purposes. First, it holds the electrolyte in place between the cathode and the anode by capillary action and prevents the molten salts from completely flooding the porous electrodes; second, the membrane acts to prevent the bulk diffusion of gases between the cathode and the anode side of the cell. Two slightly different methods of preparation were used, one for the higher gas composition (100 ppm) and another for the lower (20 ppm). The reason was simply to compare the effectiveness of the structures.

Manufacture of the membrane for the 100 ppm tests involved making a composite structure consisting of woven zirconia cloth which was densified with MgO powder. The structure consisted of a single mat of ZYW-30A zirconia cloth, 0.000 76 m thick (purchased from ZIRCAR Inc.) layered with two tapes of MgO ceramic powder suspended within acrylic binder K565-4 (purchased from Metoramic Sciences, Inc.). An oxygen sweep was applied to both sides of the cell and the cell was loaded into the furnace for heat-up. The binder from the MgO tapes was burned out at 648 K overnight. The temperature was then ramped up to run temperature and the electrolyte was wicked into the MgO powders and zirconia cloth. Process gas was then supplied to the cell and the electrolyte was allowed to reach the equilibrium described by Reaction 5.

For the lower-concentration inlet gases, a membrane was prepared from a 0.000 76 m thick zirconia cloth which was rigidized to 60.8% voids using sub-micron particles of ZrO_2 within an aqueous slurry (44 wt %). This was accomplished by cutting a 0.076 m diameter mat of zirconia cloth and soaking it in Zircar brand Rigidizer. The mat soaked the aqueous slurry into its voids and left the ZrO_2 particles behind after the H_2O was dried out. Two tapes of MgO/ZrO_2 (4 μm particle size, Aesar) in vinyl binder (B73305 Metoramics binder system) were layered on each side of the rigidized mat to further densify the structure. Other experimental details were unchanged from the high-concentration tests.

3.4. *Pre-run and analysis*

Once assembled, the cell was loaded into a custom-made furnace and connected to the process and sweep gas supply lines. The exit gas from the cathode was routed to a Beckman i.r. scanner for reading CO_2 levels and a Teledyne u.v. scanner for reading H_2S levels. A Hewlettt/Packard gas chromatograph fitted with a flame photometric detector was also used for reading H_2S levels exiting the cell. A gold reference electrode was placed on the surface of the membrane away from either process electrode and supplied with a flow of 15% CO_2/3% O_2/balance N_2 mixture to maintain a stable thermodynamic reference potential by Reaction 17:

$$CO_2 + \tfrac{1}{2}O_2 + 2e^- \longrightarrow CO_3^{2-} \qquad (17)$$

Melting of the electrolyte was verified by a sudden improvement in the seals formed by contact of the membrane with the MACOR surfaces along with observed electrical conductivity through the cell. Process gas, consisting of specified levels of CO_2, CO, H_2, H_2O, and H_2S was then supplied through the cell via a stainless steel shift reactor which allowed the water-gas shift Reaction 18, to go to equilibrium at the process temperature before the gases entered the cell:

$$CO + H_2O = CO_2 + H_2 \tag{18}$$

3.5. *Test procedure*

Once the cell had reached run temperature, conductivity across the cell was estimated by current interrupt. The equilibrium potentials at the cathode and anode were measured with respect to the reference electrode. Base-line exit cathode gas compositions were also measured at this point. Current was then applied to the cell in a stepwise fashion and the cell was allowed to equilibrate for at least 15 min after each current step. Once stabilized, potentials with respect to the reference electrode and exit gas compositions were measured.

4. Experimental results

Removal of H_2S and CO_2 from the process gas stream at the cathode and evolution of products at the anode were measured over a range of gas compositions representing sour coal gas which had been cleaned of H_2S to a level of 100 ppm to 10 ppm H_2S. Process temperature and gas flow-rates were also varied to be representative of conditions likely to be of industrial interest.

The maximum removals reported below are removals of H_2S and CO_2 on a zero current basis to compensate for any chemical scrubbing by the carbonate. H_2S removal is therefore defined as

$$\%\ \text{Removal} \equiv \left[\frac{(H_2S)_{i=0} - (H_2S)_i}{(H_2S)_{i=0}}\right]_{\text{exit}} \times 100 \tag{19}$$

Selectivity is defined by the following equation:

$$\text{Selectivity} \equiv \left[\frac{\%\ \text{Removal}_{H_2S}}{\%\ \text{Removal}_{CO_2}}\right] \times \left[\frac{(CO_2)_{\text{inlet}}}{(H_2S)_{\text{inlet}}}\right] \tag{20}$$

If selectivity is equal to one, removals of H_2S and CO_2 are equivalent. If the selectivity is greater than one, H_2S is preferentially removed.

A total of nine successful experiments were performed. Two of these are presented here; reproducibility of removal trends was observed in all nine experiments.

4.1. *Polishing application with 100 ppm H_2S in coal gas*

This experimental run used a simulated coal gas with a composition of 14.3% CO_2, 50.8% CO, 4.8% H_2O, 30.1% H_2, and 100 ppm H_2S after shift reaction. The electrodes were both lithiated NiO. The acrylic binders used in the MgO tapes (Metoramics K565-4 binder system) were burned out under an oxygen atmosphere at 623 K and the Li/K eutectic-composition electrolyte was added with the cell at run temperature. The inlet gases were passed through a stainless steel shift reactor to allow them to come to their equilibrium composition before passing through the cell.

The cell temperature was 973 K; at this temperature, analysis of the limiting current densities within the system, as outlined earlier, shows that the gas phase limiting current density for H_2S reduction was 11.5 A m^{-2} while the membrane limiting current density for sulfide transport was 32.9 A m^{-2}. This shows that the maximum flux of material through the membrane is three times greater than the maximum flux of material through the gas phase to the membrane surface. H_2S removal at a variety of flow-rates was observed and is presented here in Figs 7 to 10. Cell polarization is presented in Fig. 11; parametric numbers on this graph are cathodic flowrates in m^3 × 10^{-6} (cm^3 min^{-1}). The measured cross-cell resistance was estimated with current-interrupt and was found to be about 1 Ω. With the maximum current applied to the cell of 31 A m^{-2}, this corresponds to 0.02 V of ohmic loss. This is slight compared to the overall cross-cell potential, which includes concentration effects and other overpotentials.

An H_2S removal level of 89.2% (exit H_2S level brought from 89.5 to 9.7 ppm with applied current) was achieved. Cell current efficiency and species removal for this run are presented in Fig. 10. At only slightly above stoichiometric current, H_2S current efficiency is 40%. The remaining 60% of the 1.9 A m^{-2} applied to the cell at this point would remove only 6 ppm CO_2 from the process gas stream with 19.1% CO_2 entering the cell; such transport of CO_2 is completely negligible. At the highest applied current to the cell at the cathode flow-rate of 0.000 088 m^3 min^{-1}, the H_2S current efficiency is only 4.6% (Fig. 10); the concurrent removal of CO_2 results in a drop in CO_2 of only 0.17%. The selectivity for H_2S is thus of the order of 10^5.

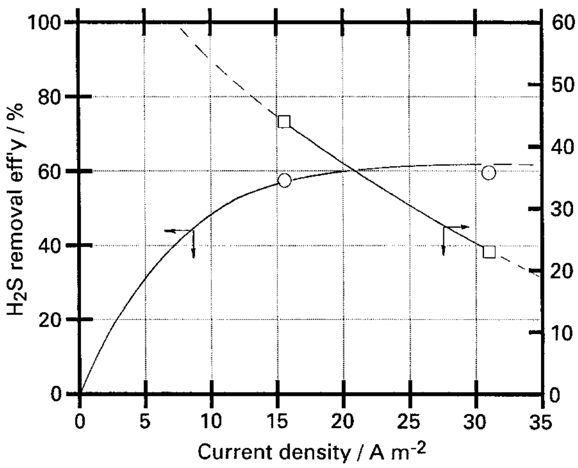

Fig. 7. H_2S removal and efficiency against applied current density. 100 ppm H_2S, 600 × 10^{-6} m^3 min^{-1}.

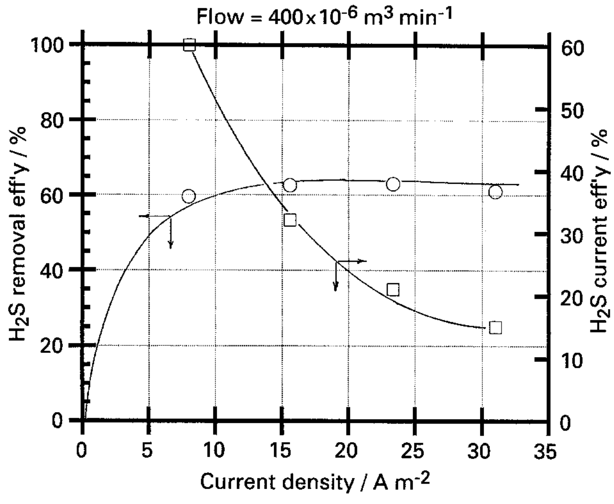

Fig. 8. H_2S removal and efficiency against applied current density. 100 ppm H_2S, 400 × 10^{-6} m^3 min^{-1}.

The theoretical *maximum* current efficiency for this system at 89% removal of H_2S would be approximately 35%, as shown in Fig. 3. The reason for the difference between the observed and theoretical current efficiencies is due to slight H_2 crossover, as discussed earlier. It should be recognized that less than 0.5% of the H_2 at the cathode is needed to cause this effect. The excess current is used to reduce CO_2 (and H_2O) by Reaction 4, and to oxidize carbonate by Reaction 13. Improvements in membrane gas-permeability will act to sharply lower the extent of this reaction path.

4.2. *Polishing application with 20 ppm H_2S in coal gas*

The lower-concentration tests were run in a manner similar to those with 100 ppm gas. The run temperature was 923 k. After binder burnout and electrolyte melting, fuel gas of composition 15.2% CO_2, 44.2% CO, 5.4% H_2O, 35.0% H_2 (after shift reaction) with 18.8 ppm H_2S was put through the cell. This gas composition and temperature gives an estimated equilibrium-membrane-sulfide level of 0.06 mol % sulfide.

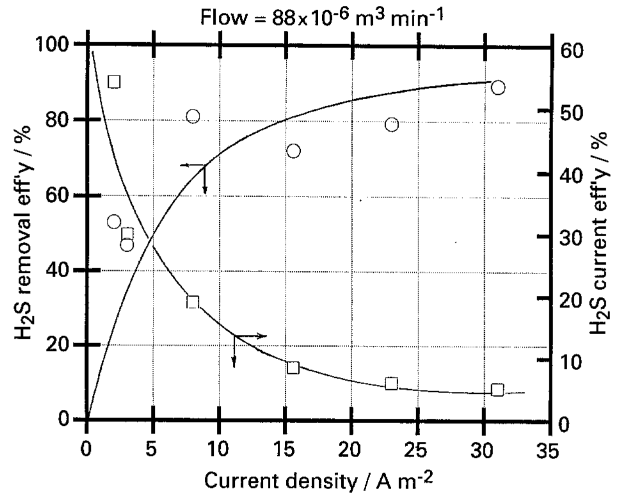

Fig. 10. H_2S removal and efficiency against applied current density. 100 ppm H_2S, 88 × 10^{-6} m^3 min^{-1}.

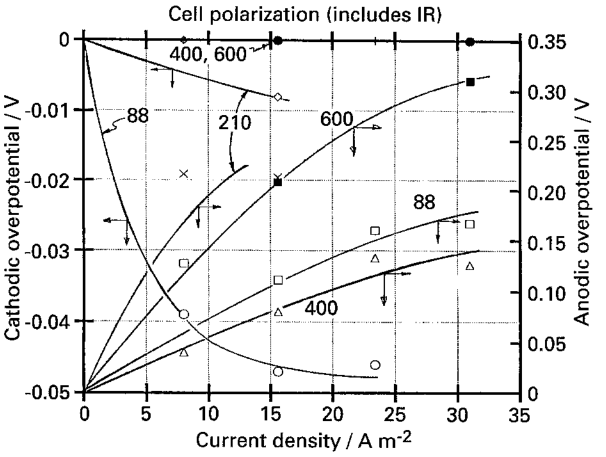

Fig. 11. Cell polarization against applied current. 100 ppm H_2S, parametric numbers are cathodic flowrate × 10^{-6} m^3 min^{-1}.

The gas phase limiting-current density was estimated to be 1.8 A m^{-2} and the membrane limiting current density was 3.4 A m^{-2}.

H_2S removal data were taken at a variety of cathodic flow rates. Current efficiency and species removal for this run are presented in Fig. 12. H_2S levels were brought from 15.8 ppm exiting the cell

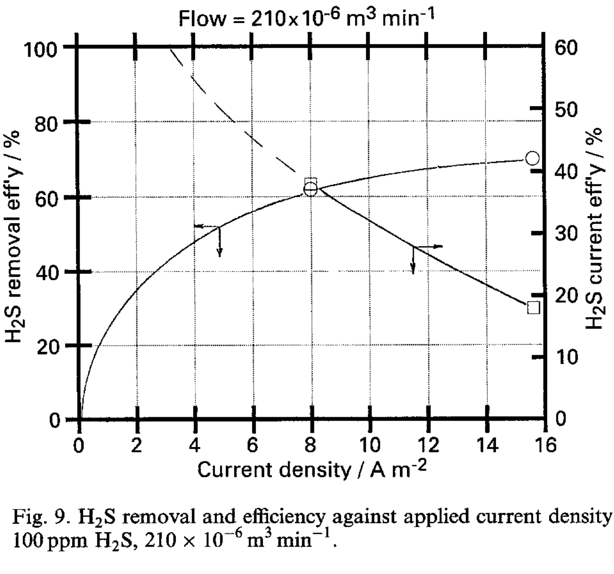

Fig. 9. H_2S removal and efficiency against applied current density. 100 ppm H_2S, 210 × 10^{-6} m^3 min^{-1}.

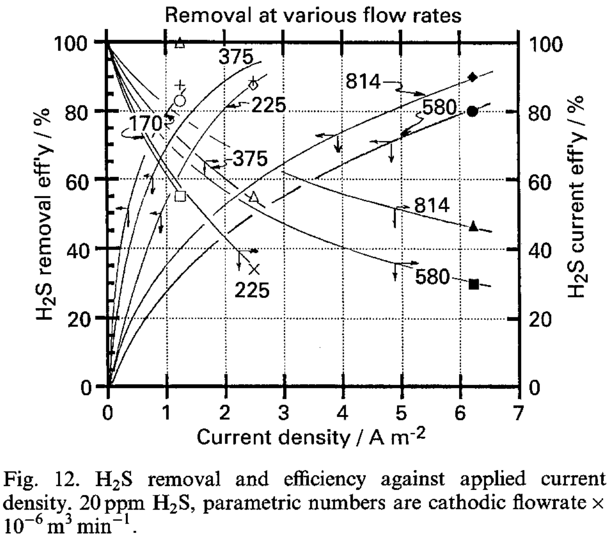

Fig. 12. H_2S removal and efficiency against applied current density. 20 ppm H_2S, parametric numbers are cathodic flowrate × 10^{-6} m^3 min^{-1}.

with no current applied, to 4 ppm H_2S with 6.3 A m^{-2} applied. The selectivity of this membrane was high (selectivity the order of 10^6), but some CO_2 transport was observed. H_2S current efficiency was surprisingly higher than seen in the higher-concentration runs. This is no doubt due to improved resistance to H_2 crossover through this membrane.

5. Economic projection

Accurate cost figures for processes early in development are impossible to project. However, it is possible to roughly estimate the power and capital requirements to assess viability. The power assumption has been shown to be overwhelmingly due to cell current, which is near stoichiometric. Cell voltage, as shown earlier, can be estimated with reasonable accuracy. Capital costs can be estimated by analogy with MCFC stacks, whose design these cells will mimic.

The proposed electrochemical membrane separator (EMS) system design, Fig. 13, is compared to a Sulfinol process with a Claus plant for sulfur recovery. The base case is provided in a discussion of coal gas processing economics by Oak Ridge National Laboratory (ORNL-5425) [14]. The medium-Btu gas treating facility discussed here treats 590 million kg h^{-1} of coal synthesis gas with composition outlined in Table 3. The capital cost for a Sulfinol plant consisting of two parallel units was estimated as 39.4 MM$ in the first quarter of 1978. This scales to 145 MM$ in mid-1987 dollars using Marshall–Swift cost indexes [15]. This does not include costs for cooling the gas stream from gasification temperatures (~ 1023 K) to Sulfinol process temperature (311 K) or the cost of reheating the gas for feed to the turbines of a cogeneration power plant or an MCFC power plant.

The acid gas stream generated by the Sulfinol plant has an H_2S level of 28.5 vol %. This is fed to a Claus plant capable of handling a load of 247 metric tonnes per day of sulfur production. The Claus plant for treating this acid gas had an estimate capital cost of 8 MM$ in 1978 dollars. This scales to 29.4 MM$ in 1987 dollars by Marshall–Swift indexes. The combined Sulfinol/Claus plant capital cost for treating this coal synthesis gas is therefore 174 MM$ in 1987 dollars (not including gas cooling and reheating costs).

Table 3. Medium heating value and coal synthesis gas composition

Gas component	Flow/kg h^{-1} × 10^{-3}	Flow/kmol s^{-1}	Vol %
H_2	92.33	12.9	68.6
N_2	14.83	0.147	0.781
CO	97.71	0.971	5.16
CO_2	64.48	0.407	2.16
H_2O	3.06	0.047	0.250
H_2S	19.97	0.163	0.866
CH_4	178.50	3.10	16.5
C_2	80.21	0.743	3.95
C_3	36.25	0.230	1.22
C_4	12.39	0.059	0.313
C_5	1.60	0.049	0.260
Total	601.33 (36.4 × 10^6 SCMD)	18.82	100.0

Pressure: 43.2 bar; temperature: 311 K; heating value: 19.1 × 10^6 J m^{-3}.

The capital cost of the EMS is more difficult to estimate than the power consumption. In the MCFC, current densities greater than 1600 A m^{-2} are routinely achieved. There are, however, two major differences between the MCFC and the EMS. In the MCFC the gases are relatively rich, as compared with the dilute reactants treated in the EMS. Further, there is no competing reaction to dilute the current carrying anion. Thus, gas-phase diffusion of H_2S or sulfide migration in the membrane may limit the current density and define the needed active membrane area for a given duty.

Gas-phase transport can be controlled through proper design of the gas channels [16]; pore diffusion in the electrodes has been found not limiting in similar designs for CO_2 removal to very low levels [17]. The limiting step for removal in this analysis is gas diffusion of H_2S to the cathode of the cell. This was found by comparison of species diffusion through the gas phase to species diffusion through the molten salt electrolyte. The capital cost estimation assumes that the membranes are available as 1.2 m by 1.2 m squares (as used in MCFC units) and are arranged in 'stacks' of parallel removal cells with the process gas equally divided to each cell. Each 'stack' removes approximately 90% of the H_2S fed to it. There is also assumed to be a series of parallel 0.003 m by 0.003 m flow channels directing gas flow across the surface of each electrode. A break-down of the costs associated with the EMS stacks is provided in [18]. For an EMS system operating at a pressure of 42.7 atm at gasification temperatures of 1023 K, the limiting current density for the first stack (which removes H_2S from 0.9% to 900 ppm) is 1130 A m^{-2}. The second stack (900 ppm to 90 ppm H_2S) has a limiting current density of 113 A m^{-2}. The third stack (90 ppm to the final H_2S level of 6 ppm) has a limiting current density of 10.0 A m^{-2}.

As soon as the limiting current density of the stack is known, the total stack area (or number of cells in the stack) can be calculated by dividing the required stack current by the stack limiting current density. The H_2S stack current is assumed to be stoichiometric for the moles of H_2S removed. The total molar flow rate to be treated by the EMS system is 18.8 kmol s^{-1}. Thus, the H_2S current applied to the first stack (0.9% to 900 ppm H_2S) is 2.82×10^7 A, the second stack (900 ppm to 90 ppm H_2S) requires 2.94×10^6 A, and the third stack (90 to 6 ppm H_2S) requires 3.05×10^5 A. For the first stack, with $I_{H_2S} = 2.82 \times 10^7$ A and $i_{d,H_2S} = 1133$ A m^{-2}, the total active membrane area is 24 889 m^2. If 1.2 m^2 by 1.2 m^2 membranes are used in this application, this comes to 17 284 electrochemical cells in the first

Table 4. Breakdown of capital investment for CG EMS (1987 $US)

Items	*Electrochemical membrane separator cell stacks/$ × 10^6* *Stack 1*	 *Stack 2*	 *Stack 3*
Ion exchange area/ $m^2 \times 10^3$	24.9	26.0	30.5
Membranes in stack	17 284	18 036	21 210
Anodes	2.299	2.402	2.824
Cathodes	0.948	0.991	1.164
Bipolar hardware	1.733	1.811	2.129
Membranes	0.107	0.112	0.131
Auxiliaries	0.542	0.566	0.666
Assembly	2.083	2.176	2.558
Stack cost	7.712	8.058	9.472
Rectifier	4.195	4.383	5.153
Controls and misc.	5.845	6.107	7.180
Assembly	4.600	4.807	5.651
Total stack cost	22.35	23.36	27.46
Total EMS cost		73.17	
Blowers		0.101	
Heat exchangers		negligible	
Plant cost		73.27	
Project contingency (15%)		10.99	
Fixed capital investment		84.26	

stack. The active membrane area of the second stack is 25 971 m^2 (18 036 cells), and the active membrane area for the third stack is 30 543 m^2 (21 210 cells).

Stack power requirements depend on the total current driving the H_2S removal and the cross-cell potential of the removal cell. Because of parallel CO_3^{2-} transport, current levels greater than stoichiometric H_2S removal current are required. By the analysis presented earlier in this paper, current efficiency at 90% H_2S removal was found to be 89.1% in the first stack with a cross cell potential of 0.764 V. At this current efficiency, the first stack requires 24 180 kW. The second stack has a current efficiency of 81.6% with a cross cell potential of 0.665 V; at these conditions this translates to 2396 kW required by the stack. The third stack has a current efficiency of 51.6% and a cross cell potential of 0.611 V; at these conditions the third stack requires 361 kW. This sums to 26 937 kW for the entire system. In these calculations, cell resistivity was estimated to be $2.5 \times 10^{-5}\,\Omega\,m^2$ after MCFC results for tape-cast electrolyte membranes of 5.0×10^{-4} m thickness and containing 40 wt % electrolyte [19].

The system costs for the EMS plant are listed in Table 4. Note in Fig. 13 that there is no need for heating the coal synthesis gas stream since the coal gasification EMS plant operates at gasification temperatures. There is, therefore, no need for a regenerative heat exchanger system to cool for H_2S removal and reheat the gas for use in a cogeneration power plant or MCFC. Since sulfur condenser costs are negligible compared to electrochemical cell stack costs, there are effectively no heat exchanger costs for this plant. An overall operation cost comparison is shown in Table 5. Note that even with the lower current efficiencies in the polishing steps of the process, the treating cost per 1000 SCM of gas treated are still competitive (in fact, even if the power requirements were doubled, the comparatively low capital investment of the proposed technology compared to the conventional technology still provides favourable economics). The overall operation cost of the two facilities was estimated after the method reported by Maddox [20]. The utilities cost and sulfur credit used in this comparison are the same as used in a previous natural gas treating plant analysis by Fluor Technology, Inc. [21].

The net treating cost presented in ($5.644/1000 SCM for conventional technology compared to $2.192/1000 SCM for the proposed EMS technology) refers to the cost associated with sweetening the gas and producing sulfur. The addition of several plant areas would be required to develop a total cost-of-gas treating. That is, the 'net treating cost' presented here relates only to the systems described and should be used only to establish the relative economic merits of the proposed EMS technology for selective H_2S removal. Once again, the conventional cost of gas treating presented here does not include the cost of cooling the gas for removal of H_2S and reheating the gas to gasification

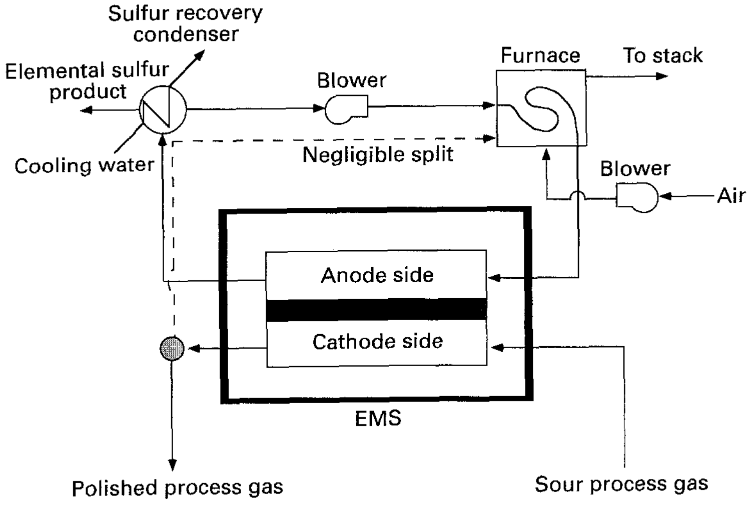

Fig. 13. Proposed coal gas sweetening EMS plant layout.

Table 5. Operation cost comparison, CG EMS to Sulfinol (1987, $US)

	Sulfinol	*EMS*
Fixed capital investment/$US × 10^6	174.4	84.26
Direct operations costs:		
Utilities/$ × 10^6		
Steam (@ $5.38/1000 kg)	7.379	0.000
Electricity (@ $0.0524/kW h)	2.076	12.20
Raw H_2O (@ $0.198/$m^3$)	8.456	0.610
Gas losses (@ $77.1/1000 SCM)	0.000	0.000
Chemical losses	1.307	0.000
	19.22	12.81
Additional costs:		
Operating labour (@ $10.30/h)	0.180	0.089
Maintenance (@ 4% FCI)	6.976	3.370
Plant general (@ 40% labour)	0.072	0.036
	7.228	3.495
Total operating costs	26.45	16.31
Indirect operating costs:		
Depreciation (@ 10% FCI)	17.44	8.426
Tax and insurance (@ 2.5% FCI)	4.360	2.107
Total indirect cost	21.80	10.53
Cost of profit (@ 25% FCI):		
(Includes income tax, interest on investment, and reasonable profit)	43.60	21.07
Grand total treating cost	91.85	47.91
Sulfur credit (@ $98/metric tonne)	−17.89	−17.89
Net treating cost:		
(Grand total − credit)	73.96	30.03
Treating cost/1000 SCM	**$5.644**	**$2.292**

temperatures after treatment. A step which would not be necessary with the proposed EMS technology.

6. Conclusions

Selective removal of H_2S has been demonstrated for polishing application to a coal synthesis gas (100 ppm H_2S) and for a purification application to coal synthesis gas (10 ppm H_2S). Electrochemical scrubbing of H_2S from coal synthesis gas at levels higher than 100 ppm has already been shown by Weaver [3, 12, 13].

The economic study presented in the previous section showed that the proposed technology is economically favourable as a method of coal gas sweetening. The results of the coal gas analysis shows that a 36.4×10^6 SCMD coal gas sweetening plant can be operated for $2.192/1000 SCM using proposed technology, as compared to $5.644/1000 SCM using conventional technology. The removal results reported here support the design specifications for the last two removal cell stacks in the coal gas plant (more concentrated H_2S coal gas streams were studied previously by Weaver).

Acknowledgements

Economic support and additional expertise were provided by the Electric Power Research Institute (EPRI) and the US Department of Energy.

References

[1] J. Winnick, 'Advances in Electrochemical Science and Engineering', Vol. 1 (edited by H. Gerischer and C. Tobias), VCH Publishers, Weinheim (1990) p. 205.

[2] H. Lim and J. Winnick, *J. Electrochem. Soc.* **131** (1984) 562.

[3] D. Weaver and J. Winnick, *ibid.* **139** (1992) 492.

[4] S. Alexander and J. Winnick, *AIChE J.*, **40** (1994) 613.

[5] D. McHenry and J. Winnick, *ibid.*, **40** (1994) 143.

[6] R. Probstein and R. Hicks, 'Synthetic Fuels', McGraw-Hill, New York (1982) p. 124.

[7] A. More, 'Sulfur, Sulfur Dioxide, and Sulfuric Acid', Verlag Chemie International Inc., Deerfield Beach, FL (1984) p. 30.

[8] US Department of Energy, 'Fuel Cells: A Handbook', DOE/METC-88/6090, Morgantown, WV (1988) p. 8.

[9] E. Banks and J. Winnick, *J. Appl. Electrochem.* **16** (1986) 583.

[10] K. White and J. Winnick, *Electrochem. Acta* **30** (1985) 511.

[11] S. Alexander and J. Winnick, *J. Sep'n Sci. Tech.* **25** (1990) 2057.

[12] D. Weaver and J. Winnick, *J. Electrochem. Soc.* **134** (1987) 2451.

[13] *Idem, ibid.* **136** (1989) 1679.

[14] Oak Ridge National Laboratory, ORNL-5425, 'Coal Gasification Processes: Energy Technology Review No. 70', Noyes Data Corp., Park Ridge, NJ (1981) p. 290.

[15] Marshall and Swift Publ., Co., *Chem. Eng.* **94**(4) (1987) 7.

[16] D. Townley and J. Winnick, *IEC Proc. Des.* **20** (1981) 435.

[17] M. Kang and J. Winnick, *J. Appl. Electrochem.* **15** (1985) 431.

[18] A. Appleby and F. Foulkes, 'Fuel Cell Handbook', Van Nostrand Reinhold, New York (1989) p. 574.

[19] R. Petri and T. Benjamin, Proc. 21st Intersociety Energy Conversion Engineering Conference, Vol. 2, ACS, Washington, DC (1986) 1156.

[20] R. Maddox, 'Gas and Liquid Sweetening', 2nd edn, Campbell Petroleum Series, Norman, OK (1977) p. 235.

[21] Fluor Technology Inc., 'Fluor Contract 842304', personal communication with D. Borio, ABB/Combustion Engineering, Windsor, CT (1990).

[22] F. Incropera and D. DeWitt, 'Fundamentals of Heat and Mass Transfer', 2nd edn, Wiley and Sons, New York (1985) p. 277.

[23] G. Prentice, 'Electrochemical Engineering Principles', Prentice Hall, Englewood Cliffs, NJ (1991).